Received: 21 November 2022 | Revised: 1 February 2023 | Accepted: 1 March 2023

DOI: 10.1002/mgg3.2169

Molecular Genetics & Genomic Medicine Open Access WILEY

ORIGINAL ARTICLE

Genetic analysis of periventricular nodular heterotopia 7 caused by a novel *NEDD4L* missense mutation: Case and literature summary

Juan Liu | **Jihong Hu** | **Yaqing Duan** | **Rong Qin** | **Chunguang Guo** | **Hongtao Zhou** | **Hua Liu** | **Chunlei Liu**

Department of Rehabilitation, Hunan Children's Hospital, Changsha, China

Correspondence
Jihong Hu, Department of Rehabilitation, Hunan Children's Hospital, Ziyuan Road & No. 86, Changsha 410001, Hunan, China.
Email: hujihong2021@163.com

Funding information
Natural Science Foundation of Hunan Province, Grant/Award Number: 2021JJ70005

Abstract

Background: Neurodevelopmental disorders associated with periventricular nodular heterotopia (PVNH) are characterized by phenotypic and genetic heterogeneity. *NEDD4L* mutation can lead to PVNH7. However, at present, only eight *NEDD4L* pathogenic variants have been identified across 15 cases of PVNH7 worldwide. Given this dearth of evidence, the precise correlations between genetic pathogenesis and phenotypes remain to be determined.

Methods: This report discusses the case of a 19-month-old male child with cleft palate, seizures, psychomotor retardation, and hypotonia, for whom we verified the genetic etiology using Trio-whole-exome and Sanger sequencing to analyze the potential pathogenicity of the mutant protein structure. Mutant plasmids were constructed for in vitro analyses. After transfection into human 293 T cells, the mutant transcription process was analyzed using real-time PCR (RT-PCR), and levels of mutant protein expression were examined using western blotting (WB) and immunofluorescence (IF) experiments.

Results: Genetic analyses revealed a novel missense mutation Gln900Arg, located in the homologous to E6-APC terminal (HECT) domain of *NEDD4L* and that the parents were wild-type, suggestive of a de novo mutation. The variant was predicted to be pathogenic by bioinformatics software, which also suggested alterations in the structural stability of the mutant protein. RT-PCR results indicated that the mutation did not affect mRNA expression, whereas WB and IF results indicated that the level of mutant protein was significantly reduced by 41.07%.

Conclusion: Functional experiments demonstrated that Gln900Arg probably did not lead to transcriptional abnormalities in this patient, instead leading to increased ubiquitination activity owing to the constitutive activation of the HECT domain, thereby promoting protein degradation. Extensive clinical reports should be generated for patients presenting with PVNH and/or polymicrogyria,

developmental delay, syndactyly, and hypotonia to increase the pool of evidence related to *NEDD4L*.

KEYWORDS

genetic analysis, homologous to E6-APC terminal, NEDD4L, periventricular nodular heterotopia, ubiquitination

1 | BACKGROUND

Heterotopic gray matter is a congenital malformation in which the migration of neuroblasts from the ventricular wall to the cerebral cortex is blocked during embryonic development, causing part of the gray matter to remain permanently between the ependyma and the cortex. Its most common manifestation is periventricular nodular heterotopia (PVNH), which is characterized by the accumulation of heterotopic gray matter along the lateral ventricular wall (Guerrini & Filippi, 2005). Clinically, patients with PVNH mainly present with various types of epilepsy and different degrees of intellectual disability (Heinzen et al., 2018).

NEDD4L pathogenic variants can lead to human paraventricular nodular heterotopia type 7 (PVNH7, OMIM # 617201). Broix et al. first identified a *NEDD4L* mutation in seven patients with PVNH, including two siblings and five unrelated patients (Broix et al., 2016). At present, only eight *NEDD4L* pathogenic variants have been identified across 15 cases of PVNH7 worldwide. Common manifestations in these patients have included psychomotor retardation, intellectual disability, and hypotonia, although some patients also exhibit cleft palate and seizures (Broix et al., 2016; Elbracht et al., 2018; Kato et al., 2017; Pecimonova et al., 2021; Stouffs et al., 2020).

Notably, these *NEDD4L* pathogenic variants are mainly distributed in the homologous to E6-APC terminal (HECT) domain, which may lead to abnormal biological function owing to alterations in the domain conformation, thereby promoting autophagy and protein ubiquitination (Broix et al., 2016). However, given a dearth of evidence and reports related to PVNH7, the precise correlations between genetic pathogenesis and phenotypes remain to be determined.

In the present study, we performed a genetic analysis of a Chinese child with seizures and psychomotor retardation. A novel missense mutation (located in the HECT domain) of *NEDD4L* was detected via trio-whole-exome sequencing (Trio-WES). The mutant plasmid was constructed in vitro, and western blotting (WB) and immunofluorescence (IF) experiments indicated that the mutation resulted in reduced protein expression. Previously reported cases related to *NEDD4L* mutation are also summarized. Finally, this report focuses on the diagnostic value of gene detection in patients with early infantile epilepsy and psychomotor retardation, further enriching data related to *NEDD4L* mutation profile in the Chinese population.

2 | MATERIALS AND METHODS

2.1 | Ethics approval

This study was approved by the Medical Ethics Committee of Hunan Children's Hospital. The patient's parents provided written informed consent for disclosure of the patient's clinical manifestations, auxiliary examinations, magnetic resonance imaging (MRI) data, and gene mutation data.

2.2 | Whole-exome and sanger sequencing

First, 3 mL of peripheral blood was collected from both the proband and parents for Trio-WES detection. Subsequently, white blood cell DNA was extracted using a genome extraction kit, in accordance with the manufacturer's instructions (CoWin Biosciences). Thereafter, a genome library was constructed, and the target gene sequence was captured using the Illumina NovaSeq 6000 high-throughput sequencing platform (Illumina), covering the exon and intron junction area of single-gene diseases, including *NEDD4L*. The dbSNP (www.ncbi.nlm.nih.gov/snp), ExAC (www.exac.broadinstitute.org/), and 1000 Genomes (www.1000genomes.org) databases were used to screening the potential mutations. Online softwares [SIFT (www.sift.bii.a-star.edu.sg); Polyphen-2 (www.genetics.bwh.harvard.edu/pph2); and MutationTaster (www.mutationtaster.org) software] were used to predict and analyze the hazard of the variation spectrum, following which it was annotated in accordance with the American Guidelines for Medical Genetics and Genomics (ACMG) (Richards et al., 2015). Finally, the screened pathogenic variant was subjected to Sanger sequencing, and primers were designed in reference to the Ensemble database. The upstream and downstream primer sequence was

5′-GTGCCATCAGAGAGTTTGCTTTT-3′ and 5′-ACACT GTCCTGAAACTTAGCCTT-3′, respectively. The amplified products were sequenced using an ABI 3500 Genetic Analyzer (Applied Biosystems).

2.3 | Structural analysis of mutant protein

NEDD4L protein sequences were obtained from the National Center of Biotechnology Information (NCBI) (www.ncbi.nlm.nih.gov/nuccore/NM_001144967.3/), and a template search was performed utilizing the BLAST function provided by NCBI (www.blast.ncbi.nlm.nih.gov/Blast.cgi). A three-dimensional structural simulation was performed using multi-template modeling (template PDB: 2ONI) in MODELER v9.15 to construct the tertiary and complete structures, and the mutant structure was built on the wild-type structure using PYMOL v2.2 (www.pymol.org/2/).

2.4 | Cell culture and plasmid construction

Human 293T cells were incubated in a 5% CO_2 incubator at 37°C using 10% DMEM (Thermo Fisher Scientific, Ma, USA) for culture. Aliquots of 7×10^5 cells were plated in six-well plates 1 day in advance, and cell transfections were performed when cells were 60%–70% confluent after incubation overnight. A total of 1.5 μg of plasmid was transfected using 5 μL Lipofectamine™ 3000 (#L3000150, Invitrogen), which was switched to 10% DMEM 6 h later. The *NEDD4L* (NM_001144967) CDS region was amplified using high fidelity polymerase Phanta® Max Super-Fidelity DNA Polymerase (#P505, Vazyme) and constructed onto the vector pECMV-3×FLAG-C. The forward and reverse amplification primer sequence was 5′-CTTGGTAC CGAGCTCGGATCCATGGCGACCGGGCTCGGG-3′ and 5′-TGCTGGATATCTGCAGAATTCATCCACCCCTT CAAATCCTTG-3′, respectively, constructed onto vector pECMV-3×FLAG-C. Mutations were made using a Mut Express MultiS Fast Mutagenesis Kit V2 (Vazyme #C215; single-point mutation forward and reverse amplification primer sequence: 5′-GTATCCGGTTACTGCGG TTTGTCACA-3′ and 5′-CGCAGTAACCGGATACGCTT TTCGGC-3′, respectively).

2.5 | Real-time PCR

Total RNA was extracted from transfected cells using the Trizol reagent (Invitrogen #10296010) and subjected to further processes with a RevertAid First Strand cDNA Synthesis Kit (Invitrogen #K1622, Thermo Fisher Scientific) and Luna® Universal Probe qPCR Master Mix kit (NEB #M3003, New England BioLabs). The forward and reverse primer sequence was 5′-GACATGGA GCATGGATGGGAA-3′ and 5′-GTTCGGCCTAAATT GTCCACT-3′, respectively. The reaction conditions have been described previously (Kuang et al., 2020). Results were obtained using the $2^{-\Delta\Delta Ct}$ method (Livak & Schmittgen, 2001).

2.6 | WB analysis

Radio immunoprecipitation lysis buffer (Thermo Fisher Scientific, Ma, USA) was applied to extract the total protein of the cells after transfection. The total protein concentration was determined using a bicinchoninic acid protein detection kit (Thermo Fisher Scientific). Proteins were separated using 10% sodium dodecyl sulfate polyacrylamide gel electrophoresis and transferred to polyvinylidene fluoride membranes (Bio-Rad Laboratories). After blocking the membranes with the primary antibody (FLAG, Cell signaling Technology USA Cat. No. 8146; dilution of 1:1000) at 4°C overnight, they were then incubated with secondary antibody (anti-mouse IgG, HRP-linked antibody, CST USA Cat. No. 7076; dilution of 1:5000) at 27°C for 2 h. The target bands were finally detected using a chemiluminescent substrate (Perkin Elmer). Tanon-5200Multi (Tanon) was used for exposure imaging. Protein expression was analyzed using the ImageQuant (LAS-4000, FujiFilm) software. Bands were quantified using ImageJ software.

2.7 | IF analysis

Cells were fixed with 4% paraformaldehyde in Petri dishes for 15 min, following which they were blocked using a blocking solution containing Triton X-100 (T8787, Sigma-Aldrich) for 60 min at 27°C. The blocked cells were incubated overnight at 4°C with Rabbit anti-human NEDD4L (#13690-1-AP, Proteintech) at a dilution of 1:200, washed three times with phosphate-buffered saline (PBS), and incubated with conjugated goat anti-rabbit IgG (#SA00013-4, Proteintech) at a dilution of 1:100 for 1 h at 27°C in the dark. DAPI (#C1005, Beyotime) was used for staining after three washes in PBS, followed by another three washes with PBS after 5 min of incubation at room temperature. Cells were observed using laser confocal microscopy (#LAS SP8, Leica Microsystems). The mean fluorescence intensity of target protein in cells was analyzed using the ImageJ software.

3 | RESULTS

3.1 | Case presentation

The patient was a 19-month-old male (G3P2) with no adverse prenatal or perinatal history. He had a history of pathological jaundice at birth. Seizure-like symptoms were first observed at the age of 3 months, manifesting as follows: the eyes deviated to the left and the limbs became stiff and spastic for several minutes, following which the symptoms resolved. At the age of 9 months, twitching symptoms appeared again, manifesting as follows: the eyes turned upward and whole-body convulsions were observed for approximately 1 min.

At admission, his physical examination revealed a cleft palate without other facial abnormalities, and he exhibited a height of 73 cm (−4 standard deviations [SDs]) and weight of 7.5 kg (−4 SDs). Examination also revealed poor adaptability, active grasp in both hands, and slight delays in functional motor ability. He exhibited a poor ability to raise his head in the prone position, unstable sitting posture, and low muscle tension in the limbs.

Video electroencephalography suggested a slight slowing of the background rhythm. Head MRI revealed widening of the bilateral frontotemporal extracerebral space, as well as bilateral enlargement of the lateral ventricles. PVNH was not found (Figure 1a–d). The results of the Gesell Development Scale indicated that there were moderate to severe developmental delays in motor ability, fine motor ability, adaptive behavior, speech ability, and personal social behavior. No abnormalities in blood or urine metabolites were detected. The parents of the patient were in good health and denied consanguineous marriage and family genetic disease history.

3.2 | WES identified a *NEDD4L* mutation (Gln900Arg)

The proband had a missense mutation in *NEDD4L* (NM_001144967:c.2699A>G [p.Gln900Arg]), and his

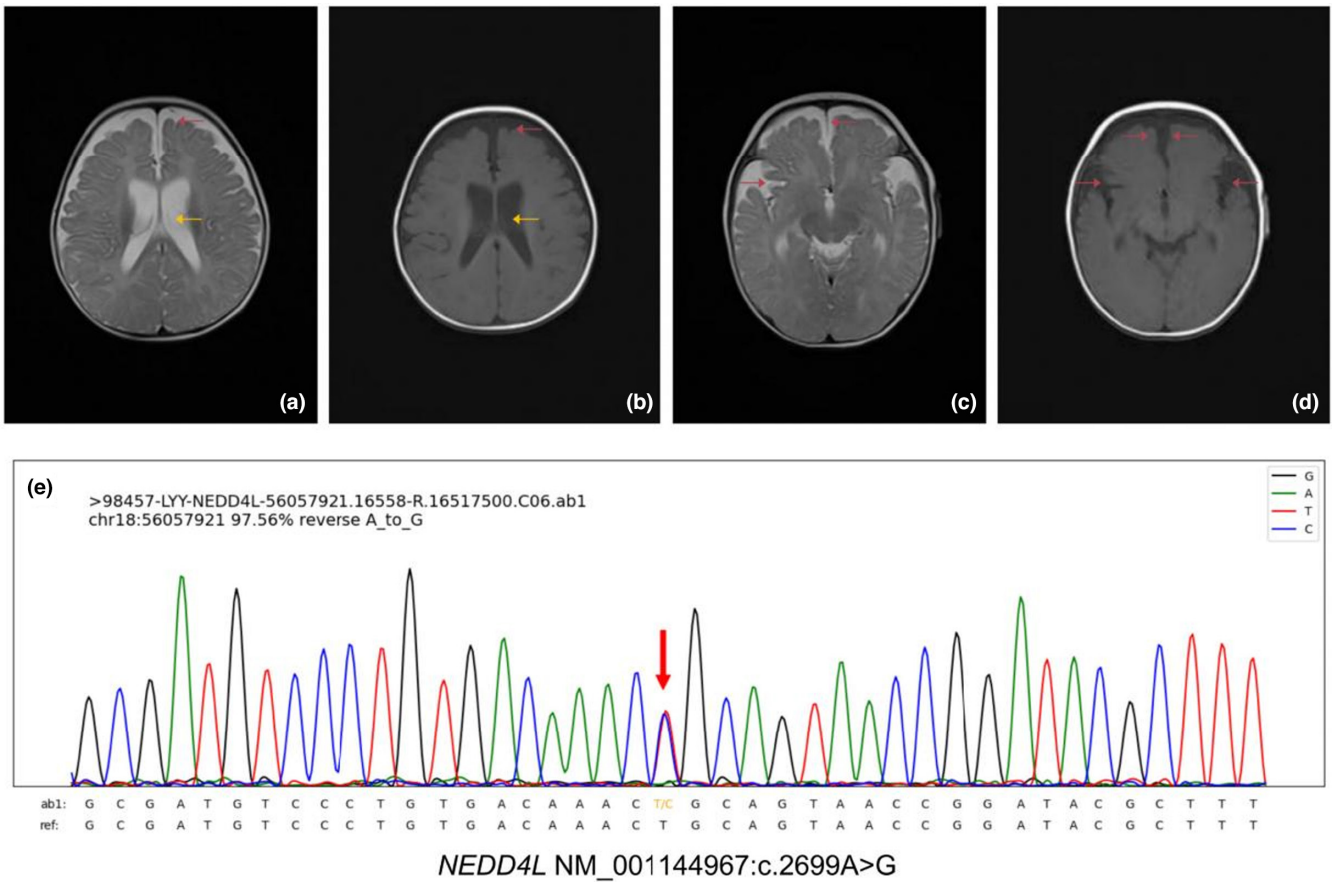

FIGURE 1 Phenotype and variation information for a 19-month-old male patient. (A–D) Head MRI revealed widening of the extracerebral space in the frontotemporal area, as well as effusion (red arrow). Panels A and B show widening of the lateral ventricle (yellow). (A) and (C) show high signal on T2-weighted imaging. (B) and (D) show low signal on fluid-attenuated inversion recovery sequences. (E) Genetic testing revealed heterozygous mutation of *NEDD4L* in the proband, NM_001144967:c.2699A>G (p.Gln900Arg).

parents were wild-type at the locus. This mutation was not included in the dbSNP, ExAC, or 1000 Genomes databases. Bioinformatic algorithms predicted that this mutation may affect protein structure/function (see Table 1 for specific algorithm species and results). Gln900arg was graded as likely pathogenic according to ACMG guidelines. Finally, Sanger sequencing confirmed the presence of this mutation in the proband (Figure 1e).

3.3 | The novel Gln900Arg mutation may lead to an altered protein conformation

The NEDD4L protein consists of HECT, 4 tryptophan (WW), and C2 domains (Escobedo et al., 2014). Gln900 is located on the α-helix of the HECT domain, and Gln900Arg occupies a larger spatial structure because the side chain is guanidinium, which forms stronger hydrophobic interactions with surrounding residues and a new hydrogen bond with Asn846. Thus, the mutation may increase the local structural rigidity, which, in turn, interferes with the protein's ability to interact with the substrate (Figure 2).

3.4 | The novel Gln900Arg mutation did not significantly affect mRNA expression

The RT-PCR results suggested a significant increase in mRNA expression in the NEDD4L experimental group (NEDD4L-WT and NEDD4L-MUT) when compared with the level observed in the empty vector control ($p = 0.025$), although there was no significant difference between NEDD4L-WT and NEDD4L-MUT ($p = 0.40$; Figure 3a). This finding indicates that the novel *NEDD4L* mutation Gln900Arg may not affect mRNA expression.

3.5 | The novel Gln900Arg mutation reduces NEDD4L protein expression

WB results suggested that NEDD4L protein expression levels were significantly higher in the NEDD4L-WT group than in empty vector controls ($p < 0.001$). However, NEDD4L-MUT significantly reduced ($p < 0.001$) the level of protein expression by 41.07% when compared with NEDD4L-WT (Figure 3b).

IF results suggested that fluorescence intensity was significantly higher for NEDD4L-WT than for NEDD4L-MUT and empty vector controls, whereas it was similar between the NEDD4L-MUT and empty vector controls (Figure 4), consistent with WB findings. Collectively, these results demonstrate that the novel Gln900Arg mutation identified in this study leads to reduced protein expression, suggesting that the mutation located in the HECT domain of the NEDD4L protein may lead to protein instability.

4 | DISCUSSION

PVNH is phenotypically heterogeneous and is often associated with epilepsy, intellectual disability, and neurological disorders. The pathogenesis of PVNH is complex, with germline genetic mutation regarded as a major contributor (Chang et al., 2007; Heinzen et al., 2018; Mandelstam et al., 2013). In the present study, the patient mainly presented with seizures, severe growth delays, and psychomotor retardation, which is very similar to findings

TABLE 1 Predicted results of mutation with different algorithms.

Gene	NEDD4L	
Transcription	NM_001144967	
Variation	c.2699A>G (p.Q900R)	
Algorithm	score	Prediction
SIFT	0	Damaging
Polyphen-2_HDIV	0.996	Probably_damaging
Polyphen-2_HVAR	0.983	Probably_damaging
MutationTaster	1	Disease_causing
PROVEAN	−3.71	Damaging
REVEL	0.742	Damaging
ACMG	Likely pathogenic	
Evidence	PM2_Supporting+PS2_Supporting +PP3(REVEL)+PP2+PM1	

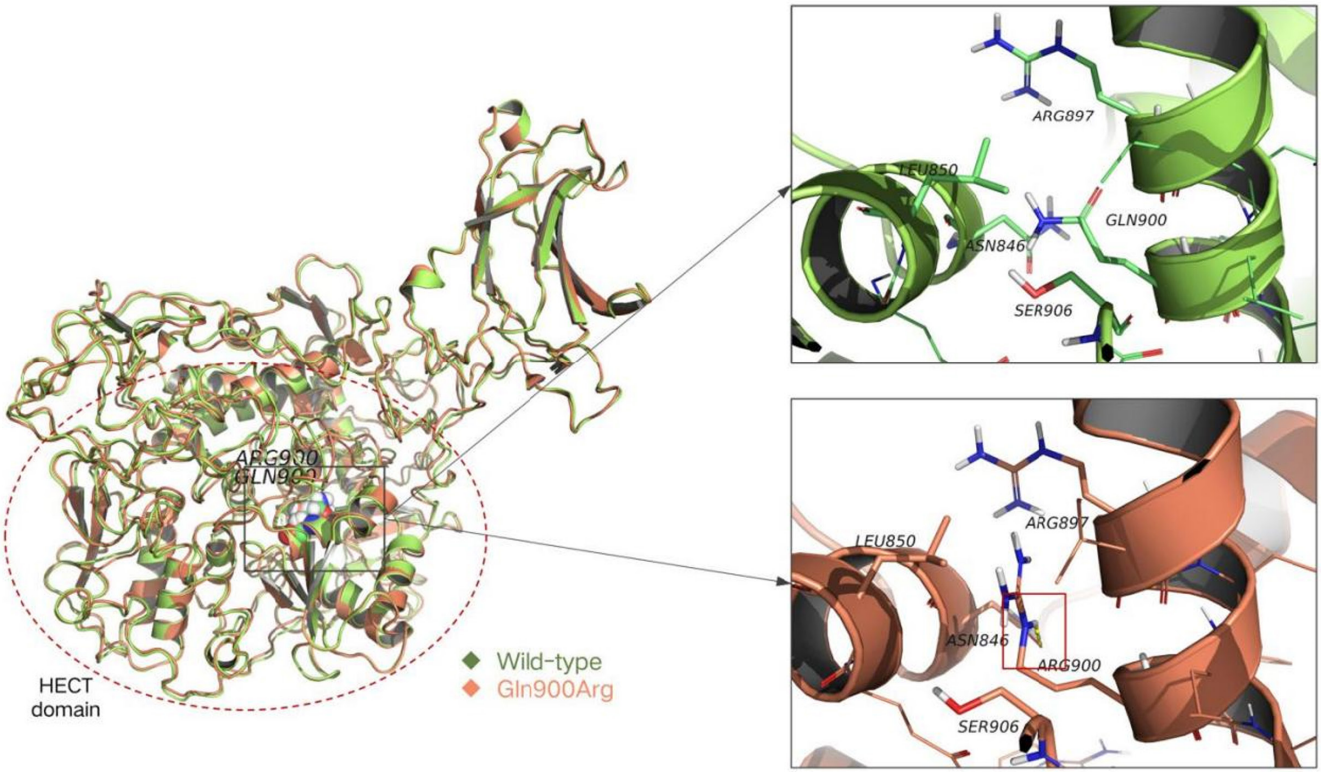

FIGURE 2 The Gln900Arg mutation occurs in the HECT domain of NEDD4L protein (red oval on the left). As the arginine side chain guanidine forms a strong hydrophobic interaction with its surroundings, forming a new hydrogen bond with Asn846 (red box on the lower right), this may lead to increased rigidity of the local structure of the protein, thereby altering the biological function of the protein.

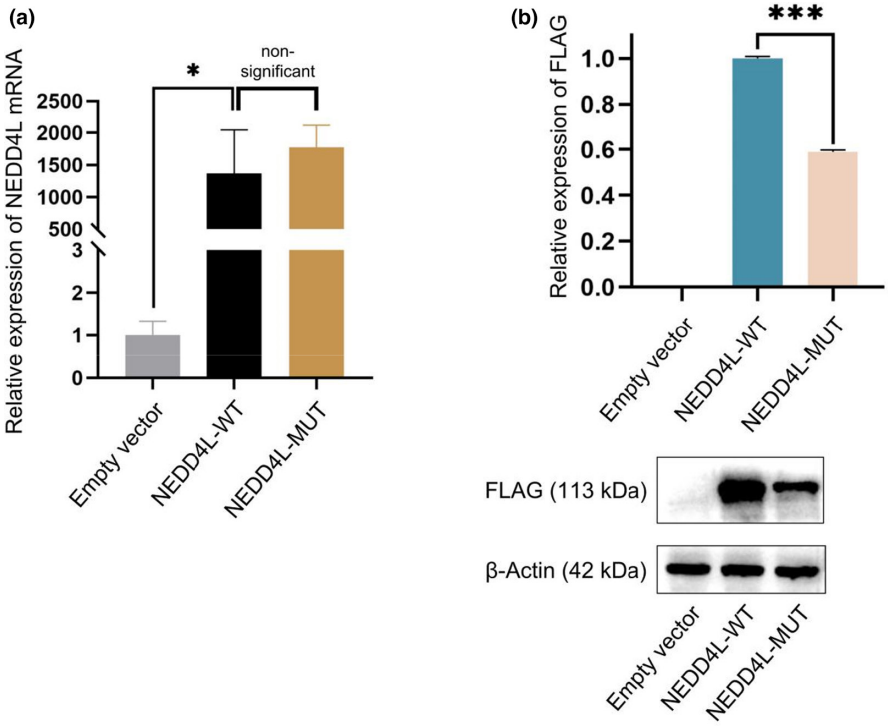

FIGURE 3 Results of mRNA transcription and protein expression. (A) mRNA expression was detected in the wild-type (NEDD4L-WT) and mutant (NEDD4L-MUT) groups. *NEDD4L* mRNA levels were lower in the NEDD4L-MUT group than in the NEDD4L-WT group, but this difference was not significant. $^{*}p < 0.05$. (B) Western blotting experiments revealed that expression of the wild-type protein (NEDD4L-WT) was significantly higher than that of the mutant protein (NEDD4L-MUT) and empty vector control. However, its expression was significantly lower in the NEDD4L-MUT group than in the NEDD4L-WT group (decrease of 41.07%). $^{***}p < 0.001$.

observed in patients with epileptic encephalopathy (Sun et al., 2021). Genetic testing results suggested the presence of a Gln900Arg mutation in *NEDD4L*, which, in turn, leads to the development of PVNH7.

After reviewing data from previously reported cases (Broix et al., 2016; Elbracht et al., 2018; Kato et al., 2017; Pecimonova et al., 2021; Stouffs et al., 2020), we observed that nearly all 15 patients (seven male, eight female) in the

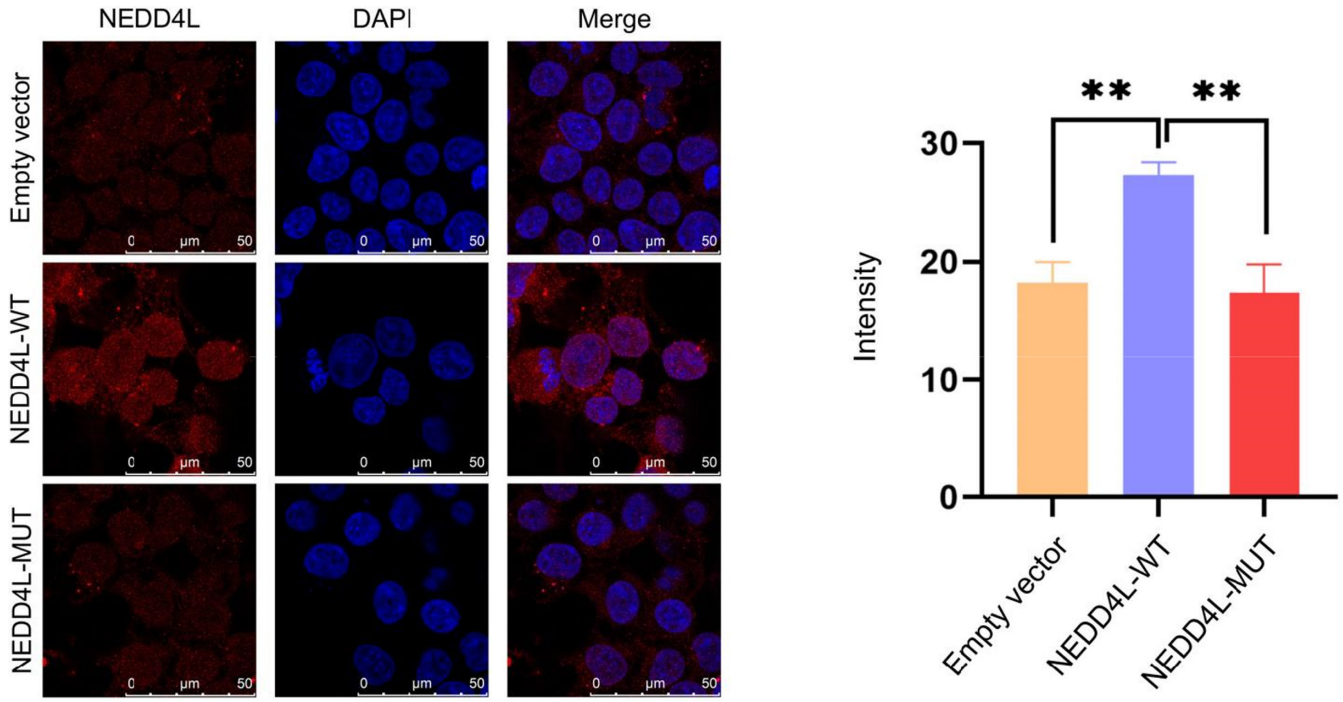

FIGURE 4 Immunofluorescence experiments indicated that fluorescence intensity in the cytoplasm was stronger in the wild-type (NEDD4L-WT) group than in the mutant (NEDD4L-MUT). Fluorescence intensity was similar for the NEDD4L-MUT and empty vector groups. Original magnification: ×650. $^{**}p < 0.01$.

11 reported families presented with psychomotor retardation, hypotonia, and variable degrees of syndactyly (usually second/third toe). Among them, 53% also exhibited cleft palate, while 46% experienced seizures. Previously reported imaging features included bilateral or unilateral PVNH, with 33% exhibiting polymicrogyria. Other abnormal findings were audiovisual dysfunction, aphasia, macrocephaly, hypospadias, and congenital heart disease (Table 2). While syndactyly and cleft palate are usually observed at birth or in the neonatal period in patients with *NEDD4L* mutation, they can be clinically difficult to distinguish given their associations with neurological disease and low phenotypic specificity. However, patients will experience gradual psychomotor and growth retardation over time. Some children will have their first seizure in infancy, and antiepileptic therapy, including in the present patient, has generally been ineffective (Broix et al., 2016; Stouffs et al., 2020). Notably, PVNH was not diagnosed during imaging of this patient, which may be related to the young age of the patient, highlighting the need for follow-up MRI.

A total of 13 loci have been associated with the development of PVNH to date, with *FLNA* pathogenic variants being the most common. Other pathological genes include *ARFGEF2*, *FAT4*, *DCHS1*, *EML1*, *INTS8*, *EML1*, *AKT3*, *MCPH1*, *ERMARD*, *MAP1B*, *ARF1*, and *NEDD4L* (Alcantara et al., 2017; Broix et al., 2016; Cappello et al., 2012; Conti et al., 2013; Fox et al., 1998; Ge et al., 2016; Heinzen et al., 2018; Kielar et al., 2014; Oegema et al., 2017; Sheen et al., 2004; Trimborn et al., 2004). Human *NEDD4L* (previously named *NEDD4-2*) is located at 18q21.31. The encoded NEDD4-like E3 ubiquitin protein ligase is a regulatory protein involved in the central nervous system that also plays key roles in embryonic mesenchymal structural differentiation and function, best known for its role in regulating the epithelial sodium ion channel (Ekberg et al., 2014; Xie et al., 2021). *NEDD4L* defects can cause a genetic hypertensive disorder known as Liddle's syndrome by increasing epithelial sodium ion channel activity (Lifton et al., 2001). Nonetheless, the regulatory roles of NEDD4L in neurodevelopment remain poorly understood. Broix et al. (2016) suggested that the mechanism by which *NEDD4L* pathogenic variants lead to PVNH may involve disruption of the AKT/mTOR and TGF-β/Smad2/3 signaling pathways. This assumption suggests that the variable phenotypes of *NEDD4L*-related disease are associated with abnormalities in its multiple potential substrates, leading to different effects in different signaling pathways, highlighting the need for additional mechanistic studies.

Of the eight reported *NEDD4L* pathogenic variants, seven occur in the HECT domain, while only one occurs in the WW structure (Broix et al., 2016; Elbracht et al., 2018; Kato et al., 2017; Pecimonova et al., 2021; Stouffs et al., 2020). HECT is a bi-lobed domain. Lobe C contains cysteines, and lobe N interacts with ubiquitinated

TABLE 2 Phenotypes and variant data for the current and previously reported cases of PVNH7.

	Patient 1 (Broix et al., 2016)	Patient 2 (Broix et al., 2016)	Patient 2's brother (Broix et al., 2016)
Race	French	French	French
Age at diagnosis	6 years	12 years	2 years
Sex	M	F	M
Stunting	+	+	+
Seizures	−	+	+
Cleft palate	−	+	−
Syndactyly	+	+	+
Hypotonia	+	NA	NA
PNH	+	+	+
Other MRI abnormalities	−	Encephalatrophy	
Other findings	Nearsighted	Audiovisual impairment	Strabismus, cryptorchidism
Mutations	c.2690G>A (p.Arg897Gln)	c.2677G>A (p.Glu893Lys)	c.2677G>A (p.Glu893Lys)
Inheritance	De novo	Maternal mosaicism	Maternal mosaicism
Race	Japanese	Slovakian	Caucasian
Age at diagnosis	3 years	2 years	14 months
Sex	F	M	F
Developmental delay	+	+	+
Seizures	+	+	+
Cleft palate	+	+	−
Syndactyly	−	+	+
Hypotonia	+	+	NA
PNH	+	+	+
Other MRI abnormalities	PMG	PMG	PMG
Other exceptions	Patent foramen ovale, arrhythmia, facial abnormalities	Strabismus, blue sclera, aphasia, hydronephrosis, bilateral clubfoot	Macrocephaly, hypospadias
Mutations	c.2617G>A (p.Glu873Lys)	c.2677G>A (p.Glu893Lys)	c.623G>A (p.Arg208Gln)
Inheritance	De novo	De novo	De novo

Abbreviations: F, female; M, male; PMG, polymicrogyria; PVNH, Periventricular nodular heterotopia.

E2; thus, the key catalytic domain of NEDD4L is a ligase, meaning that domain mutations in HECT may lead to protein autoubiquitination and degradation (Broix et al., 2016; Maspero et al., 2013). The only reported WW domain mutation Arg208Gln was observed in two unrelated families with similar phenotypes, suggestive of a hotspot mutation (Stouffs et al., 2020). However, there do not appear to be any clear phenotypic differences between HECT and WW domain mutations among the cases reported to date, all of which involved growth delays and psychomotor retardation, syndactyly, PVNH, and polymicrogyria. Nonetheless, patients with WW domain mutations may present with more severe or early-onset and febrile seizures based on the data available for four patients. Among them, one patient was admitted to the intensive care unit after developing status epilepticus (Stouffs et al., 2020). However, given the small number of reported cases, further studies are required to determine the correlation between *NEDD4L* genotype and phenotypic severity.

The novel Gln900Arg mutation in *NEDD4L* identified in this study was predicted to be biologically deleterious based on analyses performed using multiple bioinformatics programs. In addition, in vitro functional experiments involving plasmid construction indicated

Patient 3 (Broix et al., 2016)	Patient 4 (Broix et al., 2016)	Patient 5 (Broix et al., 2016)	Patient 6 (Broix et al., 2016)	Patient 7 (Elbracht et al., 2018)
French	French	French	French	Serbia/Macedonia
4 months	4 years	8 months	6.2 years	2.7 years
F	F	F	M	F
+	+	+	+	+
−	−	+	+	−
+	+	+	+	+
+	−	+	+	+
+	+	+	+	+
+	+	+	+	+
Thin corpus callosum, frontal hypoplasia	PMG	−	−	Cortical dysplasia
Hearing loss		Audiovisual impairment	Joint curvature, cryptorchidism, facial abnormality	Adducted thumbs
c.2677G>A (p.Glu893Lys)	c.2677G>A (p.Glu893Lys)	c.2082G>T (p.Gln694His)	c.2036A>G (p.Tyr679Cys)	c.2035T>C (p.Tyr679His)
De novo	De novo	De novo	De novo	Paternal mosaicism
Caucasian	Caucasian	Caucasian	Caucasian	Chinese
23 months	/	/	/	1.6 years
F	M	M	M	M
+	+	−	−	+
+	+	+	−	+
−	−	−	−	+
+	+	+	+	−
+	NA	−	−	+
+	+	+	+	−
PMG	−	−	−	Ventricular dilatation
−	−	−	−	−
c.623G>A (p.Arg208Gln)	c.623G>A (p.Arg208Gln)	c.623G>A (p.Arg208Gln)	c.623G>A (p.Arg208)	c.2699A>G (p.Gln900Arg)
Maternal	/	Maternal	Maternal	De novo

that Gln900Arg may not affect the transcription process, which is consistent with the results of Broix et al. (2016), who reported that the mutation within the HECT domain resulted in no significant reduction in transcript levels. However, the results of WB and IF experiments suggest that the mutant protein is expressed at a significantly lower level than in the wild-type. Thus, Gln900Arg may decrease structural stability in the protein, thereby leading to alterations in biological function. Although we did not examine the ubiquitination activity of NEDD4L protein, our results were in accordance with functional studies on ubiquitination of Arg897Gln by Broix et al. (2016), who reported significant increases in ubiquitination activity relative to the wild-type despite reduced stability and expression of the mutant protein. HECT domain mutations may result in constitutive activation leading to degradation of NEDD4L and other substrates via aberrant ubiquitination (Broix et al., 2016). The Gln900Arg mutation occurs in close proximity to Arg897 and is located in the same α-helix, meaning that ubiquitination effects may be similar. This also appears to explain the failure of the mutation to affect mRNA expression despite significant reductions in protein expression in WB experiments.

5 | CONCLUSION

In this report, we discussed the clinical features of a Chinese child with PVNH7 presenting with early-onset epilepsy and developmental delays owing to a novel mutation Gln900Arg in *NEDD4L*. Comparison of the present and previously reported cases suggests that the PVNH7 phenotype consists mainly of generalized psychomotor retardation, hypotonia, syndactyly, cleft palate, PVNH, and polymicrogyria. Functional experiments demonstrated that Gln900Arg probably did not lead to transcriptional abnormalities in this patient, instead leading to increased ubiquitination activity due to constitutive activation of the HECT domain, thereby promoting protein degradation. Nevertheless, the small number of reported cases highlights the need for additional studies to determine the correlation between *NEDD4L* genotype and phenotypic severity. As such, extensive clinical reports should be generated for patients presenting with PVNH and/or polymicrogyria, developmental delay, syndactyly, and hypotonia to increase the pool of evidence related to *NEDD4L* mutations.

AUTHOR CONTRIBUTIONS

Juan Liu and Jihong Hu conceived and designed this study. Yaqing Duan, Rong Qin and Chunguang Guo were responsible for the data analysis and performed data interpretation. Hongtao Zhou, Hua Liu and Chunlei Liu were responsible for the experimental data interpretation. Juan Liu wrote the article.

ACKNOWLEDGMENTS

The author thank the patient and his parents for their generous support in this research, as well as every scholar who has helped with this research.

FUNDING INFORMATION

This research was supported by the Natural Science Foundation of Hunan Province (2021JJ70005).

CONFLICT OF INTEREST STATEMENT

The authors declare that the research was conducted in the absence of any commercial or financial relationships that could be construed as a potential conflict of interest.

DATA AVAILABILITY STATEMENT

The data that support the findings of this study are available from the corresponding author upon reasonable request.

ETHICS APPROVAL AND CONSENT TO PARTICIPATE

The study was approved by the ethics committee of the Hunan Children's Hospital. Written informed consent was provided by the participant's parents.

ORCID

Jihong Hu https://orcid.org/0000-0001-8209-225X

REFERENCES

Alcantara, D., Timms, A. E., Gripp, K., Baker, L., Park, K., Collins, S., Cheng, C., Stewart, F., Mehta, S. G., Saggar, A., Sztriha, L., Zombor, M., Caluseriu, O., Mesterman, R., Van Allen, M. I., Jacquinet, A., Ygberg, S., Bernstein, J. A., Wenger, A. M., ... Mirzaa, G. M. (2017). Mutations of AKT3 are associated with a wide spectrum of developmental disorders including extreme megalencephaly. *Brain: A Journal of Neurology*, *140*(10), 2610–2622. https://doi.org/10.1093/brain/awx203

Broix, L., Jagline, H., Ivanova, E., Schmucker, S., Drouot, N., Clayton-Smith, J., Pagnamenta, A. T., Metcalfe, K. A., Isidor, B., Louvier, U. W., Poduri, A., Taylor, J. C., Tilly, P., Poirier, K., Saillour, Y., Lebrun, N., Stemmelen, T., Rudolf, G., Muraca, G., ... Chelly, J. (2016). Mutations in the HECT domain of NEDD4L lead to AKT-mTOR pathway deregulation and cause periventricular nodular heterotopia. *Nature Genetics*, *48*(11), 1349–1358. https://doi.org/10.1038/ng.3676

Cappello, S., Böhringer, C. R., Bergami, M., Conzelmann, K. K., Ghanem, A., Tomassy, G. S., Arlotta, P., Mainardi, M., Allegra, M., Caleo, M., van Hengel, J., Brakebusch, C., & Götz, M. (2012). A radial glia-specific role of RhoA in double cortex formation. *Neuron*, *73*(5), 911–924. https://doi.org/10.1016/j.neuron.2011.12.030

Chang, B. S., Katzir, T., Liu, T., Corriveau, K., Barzillai, M., Apse, K. A., Bodell, A., Hackney, D., Alsop, D., Wong, S. T., & Walsh, C. A. (2007). A structural basis for reading fluency: White matter defects in a genetic brain malformation. *Neurology*, *69*(23), 2146–2154. https://doi.org/10.1212/01.wnl.0000286365.41070.54

Conti, V., Carabalona, A., Pallesi-Pocachard, E., Parrini, E., Leventer, R. J., Buhler, E., McGillivray, G., Michel, F. J., Striano, P., Mei, D., Watrin, F., Lise, S., Pagnamenta, A. T., Taylor, J. C., Kini, U., Clayton-Smith, J., Novara, F., Zuffardi, O., Dobyns, W. B., ... Guerrini, R. (2013). Periventricular heterotopia in 6q terminal deletion syndrome: Role of the C6orf70 gene. *Brain: A Journal of Neurology*, *136*(11), 3378–3394. https://doi.org/10.1093/brain/awt249

Ekberg, J. A., Boase, N. A., Rychkov, G., Manning, J., Poronnik, P., & Kumar, S. (2014). Nedd4-2 (NEDD4L) controls intracellular Na(+)-mediated activity of voltage-gated sodium channels in primary cortical neurons. *The Biochemical Journal*, *457*(1), 27–31. https://doi.org/10.1042/BJ20131275

Elbracht, M., Kraft, F., Begemann, M., Holschbach, P., Mull, M., Kabat, I. M., Müller, B., Häusler, M., Kurth, I., & Hehr, U. (2018). Familial NEDD4L variant in periventricular nodular heterotopia and in a fetus with hypokinesia and flexion contractures. *Molecular Genetics & Genomic Medicine*, *6*(6), 1255–1260. https://doi.org/10.1002/mgg3.490

Escobedo, A., Gomes, T., Aragón, E., Martín-Malpartida, P., Ruiz, L., & Macias, M. J. (2014). Structural basis of the activation and degradation mechanisms of the E3 ubiquitin ligase Nedd4L. *Structure (London, England)*, *22*(10), 1446–1457. https://doi.org/10.1016/j.str.2014.08.016

Fox, J. W., Lamperti, E. D., Ekşioğlu, Y. Z., Hong, S. E., Feng, Y., Graham, D. A., Scheffer, I. E., Dobyns, W. B., Hirsch, B. A., Radtke, R. A., Berkovic, S. F., Huttenlocher, P. R., & Walsh, C.

A. (1998). Mutations in filamin 1 prevent migration of cerebral cortical neurons in human periventricular heterotopia. *Neuron*, *21*(6), 1315–1325. https://doi.org/10.1016/s0896-6273(00)80651-0

Ge, X., Gong, H., Dumas, K., Litwin, J., Phillips, J. J., Waisfisz, Q., Weiss, M. M., Hendriks, Y., Stuurman, K. E., Nelson, S. F., Grody, W. W., Lee, H., Kwok, P. Y., & Shieh, J. T. (2016). Missense-depleted regions in population exomes implicate ras superfamily nucleotide-binding protein alteration in patients with brain malformation. *NPJ Genomic Medicine*, *1*, 16036. https://doi.org/10.1038/npjgenmed.2016.36

Guerrini, R., & Filippi, T. (2005). Neuronal migration disorders, genetics, and epileptogenesis. *Journal of Child Neurology*, *20*(4), 287–299. https://doi.org/10.1177/08830738050200040401

Heinzen, E. L., O'Neill, A. C., Zhu, X., Allen, A. S., Bahlo, M., Chelly, J., Chen, M. H., Dobyns, W. B., Freytag, S., Guerrini, R., Leventer, R. J., Poduri, A., Robertson, S. P., Walsh, C. A., Zhang, M., & Epi4K Consortium, & Epilepsy Phenome/Genome Project. (2018). De novo and inherited private variants in MAP1B in periventricular nodular heterotopia. *PLoS Genetics*, *14*(5), e1007281. https://doi.org/10.1371/journal.pgen.1007281

Kato, K., Miya, F., Hori, I., Ieda, D., Ohashi, K., Negishi, Y., Hattori, A., Okamoto, N., Kato, M., Tsunoda, T., Yamasaki, M., Kanemura, Y., Kosaki, K., & Saitoh, S. (2017). A novel missense mutation in the HECT domain of NEDD4L identified in a girl with periventricular nodular heterotopia, polymicrogyria and cleft palate. *Journal of Human Genetics*, *62*(9), 861–863. https://doi.org/10.1038/jhg.2017.53

Kielar, M., Tuy, F. P., Bizzotto, S., Lebrand, C., de Juan Romero, C., Poirier, K., Oegema, R., Mancini, G. M., Bahi-Buisson, N., Olaso, R., Le Moing, A. G., Boutourlinsky, K., Boucher, D., Carpentier, W., Berquin, P., Deleuze, J. F., Belvindrah, R., Borrell, V., Welker, E., ... Francis, F. (2014). Mutations in Eml1 lead to ectopic progenitors and neuronal heterotopia in mouse and human. *Nature Neuroscience*, *17*(7), 923–933. https://doi.org/10.1038/nn.3729

Kuang, X., Sun, L., Wu, Y., & Huang, W. (2020). A novel missense mutation of COL4A5 gene alter collagen IV α5 chain to cause X-linked Alport syndrome in a Chinese family. *Translational Pediatrics*, *9*(5), 587–595. https://doi.org/10.21037/tp-20-47

Lifton, R. P., Gharavi, A. G., & Geller, D. S. (2001). Molecular mechanisms of human hypertension. *Cell*, *104*(4), 545–556. https://doi.org/10.1016/s0092-8674(01)00241-0

Livak, K. J., & Schmittgen, T. D. (2001). Analysis of relative gene expression data using real-time quantitative PCR and the 2(-Delta Delta C(T)) Method. *Methods (San Diego, Calif.)*, *25*(4), 402–408. https://doi.org/10.1006/meth.2001.1262

Mandelstam, S. A., Leventer, R. J., Sandow, A., McGillivray, G., van Kogelenberg, M., Guerrini, R., Robertson, S., Berkovic, S. F., Jackson, G. D., & Scheffer, I. E. (2013). Bilateral posterior periventricular nodular heterotopia: A recognizable cortical malformation with a spectrum of associated brain abnormalities. *AJNR. American Journal of Neuroradiology*, *34*(2), 432–438. https://doi.org/10.3174/ajnr.A3427

Maspero, E., Valentini, E., Mari, S., Cecatiello, V., Soffientini, P., Pasqualato, S., & Polo, S. (2013). Structure of a ubiquitin-loaded HECT ligase reveals the molecular basis for catalytic priming. *Nature Structural & Molecular Biology*, *20*(6), 696–701. https://doi.org/10.1038/nsmb.2566

Oegema, R., Baillat, D., Schot, R., van Unen, L. M., Brooks, A., Kia, S. K., Hoogeboom, A. J. M., Xia, Z., Li, W., Cesaroni, M., Lequin, M. H., van Slegtenhorst, M., Dobyns, W. B., de Coo, I. F. M., Verheijen, F. W., Kremer, A., van der Spek, P. J., Heijsman, D., Wagner, E. J., ... Mancini, G. M. S. (2017). Human mutations in integrator complex subunits link transcriptome integrity to brain development. *PLoS Genetics*, *13*(5), e1006809. https://doi.org/10.1371/journal.pgen.1006809

Pecimonova, M., Radvanszky, J., Smolak, D., Budis, J., Lichvar, M., Kristinova, D., Rozova, I., Turna, J., & Szemes, T. (2021). Admixed phenotype of NEDD4L associated periventricular nodular heterotopia: A case report. *Medicine*, *100*(22), e26136. https://doi.org/10.1097/MD.0000000000026136

Richards, S., Aziz, N., Bale, S., Bick, D., Das, S., Gastier-Foster, J., Grody, W. W., Hegde, M., Lyon, E., Spector, E., Voelkerding, K., Rehm, H. L., & Laboratory Quality Assurance Committee, A. C. M. G. (2015). Standards and guidelines for the interpretation of sequence variants: A joint consensus recommendation of the American College of Medical Genetics and Genomics and the Association for Molecular Pathology. *Genetics in Medicine*, *17*(5), 405–424. https://doi.org/10.1038/gim.2015.30

Sheen, V. L., Ganesh, V. S., Topcu, M., Sebire, G., Bodell, A., Hill, R. S., Grant, P. E., Shugart, Y. Y., Imitola, J., Khoury, S. J., Guerrini, R., & Walsh, C. A. (2004). Mutations in ARFGEF2 implicate vesicle trafficking in neural progenitor proliferation and migration in the human cerebral cortex. *Nature Genetics*, *36*(1), 69–76. https://doi.org/10.1038/ng1276

Stouffs, K., Verloo, P., Brock, S., Régal, L., Beysen, D., Ceulemans, B., Jansen, A. C., & Meuwissen, M. E. C. (2020). Recurrent NEDD4L variant in periventricular nodular heterotopia, polymicrogyria and syndactyly. *Frontiers in Genetics*, *11*, 26. https://doi.org/10.3389/fgene.2020.00026

Sun, D., Liu, Y., Cai, W., Ma, J., Ni, K., Chen, M., Wang, C., Liu, Y., Zhu, Y., Liu, Z., & Zhu, F. (2021). Detection of disease-causing SNVs/indels and CNVs in single test based on whole exome sequencing: A retrospective case study in epileptic encephalopathies. *Frontiers in Pediatrics*, *9*, 635703. https://doi.org/10.3389/fped.2021.635703

Trimborn, M., Bell, S. M., Felix, C., Rashid, Y., Jafri, H., Griffiths, P. D., Neumann, L. M., Krebs, A., Reis, A., Sperling, K., Neitzel, H., & Jackson, A. P. (2004). Mutations in microcephalin cause aberrant regulation of chromosome condensation. *American Journal of Human Genetics*, *75*(2), 261–266. https://doi.org/10.1086/422855

Xie, S., Xia, L., Song, Y., Liu, H., Wang, Z. W., & Zhu, X. (2021). Insights into the biological role of NEDD4L E3 ubiquitin ligase in human cancers. *Frontiers in Oncology*, *11*, 774648. https://doi.org/10.3389/fonc.2021.774648

How to cite this article: Liu, J., Hu, J., Duan, Y., Qin, R., Guo, C., Zhou, H., Liu, H., & Liu, C. (2023). Genetic analysis of periventricular nodular heterotopia 7 caused by a novel *NEDD4L* missense mutation: Case and literature summary. *Molecular Genetics & Genomic Medicine*, *11*, e2169. https://doi.org/10.1002/mgg3.2169